Journal of Hydroscience and Hydraulic Engineering
Vol. 16, No. 2, November, 1998, 49-62

MODELING COMPETITION AND SUCCESSION BETWEEN RED-TIDE-CAUSING *CHATTONELLA* AND DIATOMS
- ROLE OF VERTICAL MIXING AND NUTRICLINE DEPTH

By

Kunihiko Amano

Public Works Research Institute, Tsukuba 305-0804, Japan

and

Masataka Watanabe

National Institute for Environmental Studies, Tsukuba 305-0053, Japan

SYNOPSIS

We have constructed a mathematical model for describing the succession and competition between two phytoplankton species, *Chattonella antiqua* (Raphidophyceae) and *Skeletonema costatum* (diatom), to assess conditions leading to the outbreak of *C. antiqua* red tides. These two species have different characteristics but both can be the dominant species in summer depending on meteorological conditions: *C. antiqua* is a motile phytoplankton capable of diel vertical migration and nocturnal nutrient uptake. *S. costatum*, on the other hand, is non-motile and settles when mixing is suppressed. It does, however, have a higher growth rate than *C. antiqua* when placed under favorable conditions.

These characteristics are explicitly formulated in the model based on some experimental evidences presented by the existing studies. An evaluation was made of the effect of vertical mixing and nutricline depth on the two species. Simulation results showed that absence of mixing was necessary in order for *C. antiqua* to be dominant. Our model shows the potential to simulate plankton species succession under the influence of vertical mixing and nutricline depth.

INTRODUCTION

Chattonella antiqua (Raphidophyceae) red tides have often been observed since the 1960s in the Seto Inland Sea, Japan, following eutrophication there. It is known that the formation of a stable shallow (5 - 7 m) nutricline is characteristic when a *C. antiqua* red tide occurs. It is also known that a *C. antiqua* red tide often appears after several sunny and calm days in summer when vertical mixing is very weak.

When these environmental conditions prevail, *C. antiqua*, which is motile, is capable of diel vertical migration (DVM) and nocturnal nutrient uptake (16). They have an advantage over diatoms, which are not motile and tend to settle. Even if nutrients are depleted at the surface of the water where the light necessary for photosynthesis is available, *C. antiqua* can take up nutrients in a deep layer when the nutricline is shallow enough for them to access. *C. antiqua* can therefore obtain both the light and nutrients needed for growth even if they are available at the surface and at the bottom, respectively. *C. antiqua* is thought to be able to multiply sufficiently to form a red tide by exploiting this advantage (Fig. 1).

Watanabe et al. (17) have succeeded in making an artificial *C. antiqua* red tide by imposing a stable shallow nutricline in an *in-situ* enclosure

deployed in the Seto Inland Sea. Amano et al. (1) developed an ecological model for *C. antiqua* and quantitatively determined the necessary conditions for the *C. antiqua* red tide in a bay of the Seto Inland Sea.

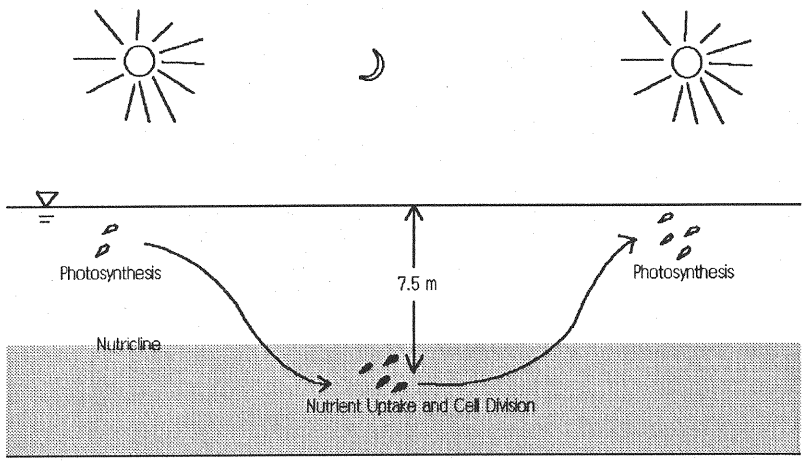

Fig. 1 Schematic figure of *C. antiqua* growth mechanism

In this paper, we present a new ecological model describing the competition between *C. antiqua* and *Skeletonema costatum*, which is a dominant diatom in the Seto Inland Sea. We examine the role of surface mixing and nutricline depth in the occurrence of the *C. antiqua* red tide in the presence of a competitor by using the model simulating different nutricline depths and mixing.

DERIVATIONS

The competitive success of *C. antiqua* seems to depend on its ability to exploit the situation in which light and nutrients are available at the surface and at the bottom, respectively. Since this situation is formed by the presence of the nutricline, which was caused by effects such as vertical surface mixing and settling of organic matter, it is essential that the model can describe variations in the vertical profiles of physicochemical parameters such as temperature and nutrient concentrations. Thus, we adopted a vertically one-dimensional model to focus on the effect of the depth of nutricline and the intensity of surface mixing on the competition between *C. antiqua* and *S. costatum*.

To describe the growth kinetics of *C. antiqua* in a bay, the model should include ecological components which deal with DVM and nocturnal nutrient uptake by *C. antiqua*, in addition to physicochemical components which calculate the surface mixing and the nutricline depth. Since *C. antiqua* is motile, it is of great importance that the model accounts for the DVM when simulating growth of the species.

There have been several studies on a model for motile plankton. Yamazaki and Kamykowski (18) used a Lagrangian approach to follow the trajectories of the cells and estimated the time history of Photosynthetically Active Radiation exposure of motile phytoplankton in the surface mixing layer. However, the number of phytoplankton cells must be limited in this approach for computational reasons, and it is difficult to apply to our study. Therefore, we adopted an Eulerian approach to describe the concentration variation of *C. antiqua* cells.

Kishi et al. (6) used an Eulerian approach for a vertically one-

dimensional model to calculate the growth of *C. antiqua* in a bay. Their model included parameters such as nutrients (orthophosphate, nitrate, inorganic iron), phytoplankton (*C. antiqua* and *Skeletonema costatum*) and zooplankton (*Paracalanus parvus*). Although their results showed that *C. antiqua* was depleted in three days even with DVM, their model of *C. antiqua* growth was different from that obtained in incubation experiments.

Since sites where *C. antiqua* red tides break out are characterized by stable stratification of salinity, temperature and nutrients in summer, the nutrient concentration which *C. antiqua* encounters varies markedly during the DVM process. In such cases, growth and nutrient uptake are unrelated (9).

It is therefore not appropriate to describe the specific growth rate by a function of the extracellular nutrient concentration. Our model employed a quota type formulation (4) to describe growth and a Michaelis-Menten model to describe nutrient uptake kinetics. This *C. antiqua* growth model is incorporated into a vertically one-dimensional diffusion model to estimate the effects of temperature, irradiance and nutrient concentrations on the growth of *C. antiqua*. The incorporation of the DVM model and the employment of a quota type formulation as the growth function make our model unique and capable of describing the ecological features of *C. antiqua* with its capability for DVM and nocturnal nutrient uptake. The DVM of *C. antiqua* is represented by a migration speed of 0.8 (m/h) when ascending from 0400 to 1700 h and descending from 1700 to 0400 h, based on field observations by Watanabe et al. (17).

Calculated variables include PO_4^{3-}, NO_3^-, NH_4^+, *C. antiqua* and *S. costatum* cell concentrations, and P and N cell quota of *C. antiqua* and *S. costatum*. Base model representing the mass balance among calculated variables is shown by Eq. 1. Changes in the phytoplankton cell concentration, intracellular nutrient concentration from nutrient uptake and cell division, and extracellular nutrient concentration are calculated in the formula account for changes in the activity of phytoplankton. Submodels for this term will be discussed in the following sections.

$$\frac{\partial C_i}{\partial t} = -\frac{1}{A}\left[\frac{\partial}{\partial z}(Q_V \cdot C_i) + \frac{\partial}{\partial z}(V_{M_i} \cdot A \cdot C_i) + \frac{\partial}{\partial z}(W_{S_i} \cdot A \cdot C_i) + \frac{\partial}{\partial z}\left(A \cdot E \cdot \frac{\partial C_i}{\partial z}\right)\right]$$

Terms for: Vertical advection DVM Settling Dispersion

$$+\{\text{change by the activity of phytoplankton}\} + \frac{U_I \cdot C_i^0}{A} - \frac{U_O \cdot C_i}{A}$$

biological production horizontal advection (1)

where

Q_V = vertical flowrate

$= \int_0^Z [U_i(z,t) - U_o(z,t)]dz$;

U_i = horizontal inflow velocity;

U_o = horizontal outflow velocity;

A_j = horizontal cross-sectional area of control volume;

C_i^0 = concentration of component i (inflow);

E = vertical dispersion coefficient;

V_M = DVM velocity (*C. antiqua* only)

= +0.8 (m/h); upward during day

= -0.8 (m/h); downward during night; and

W_S = settling velocity.

Growth model of *C. antiqua*

The growth rate for *C. antiqua* can be represented by a function of temperature, irradiation, and intracellular nutrient concentration before cell division. Functions to represent these relations are shown in Eqs. 2-8.

Detailed explanations for these equations were provided by Amano et al. (1).

(Growth function (3))

$$\begin{aligned} N &= N_0 && 04{:}00 \le t < 04{:}00 + 1\ \text{day} \\ N &= N_1 = N_0 \cdot \exp(\mu) && 04{:}00 + 1\ \text{day} \le t < 04{:}00 + 2\ \text{days} \end{aligned} \qquad (2)$$

where μ=specific growth rate;
N_0=cell concentration before division; and
N_1=cell concentration after division.

$$\begin{aligned} \mu &= f(T, I, Q^N, Q^P) \\ &= f_1(T) \cdot f_2(I) \cdot f_3(Q^N, Q^P) \end{aligned} \qquad (3)$$

(Temperature function (7))

$$f_1(T) = \left(\frac{T - T^*}{T_{opt} - T^*}\right)^n \cdot \exp\left[1 - \left(\frac{T - T^*}{T_{opt} - T^*}\right)^n\right] \qquad T^* \le T \le T_{opt}$$

$$f_1(T) = 1 - \left(\frac{T - T_{opt}}{T_{max} - T_{opt}}\right)^{m_1} \qquad T_{opt} \le T \le T_{max} \qquad (4)$$

where T^* = threshold temperature for growth;
T_{opt} = optimum temperature for growth;
T_{max} = maximum temperature for growth; and
n, m_1 = dimensionless parameters characteristic for algal species.

(Irradiation function for *C. antiqua* (2))

$$f_2(I) = \frac{i/i_k}{\left[1 + (i/i_k)^{m_2}\right]^{1/m_2}} \qquad (5)$$

where $i = I - I^*$;
$i_k = I_k - I^*$;
I^* = threshold irradiation for growth;
I_k = irradiance at which growth rate reaches a maximum; and
m_2 = dimensionless parameter characteristic for algal species.

(Specific growth rate (3))

$$\mu_N = \mu_N^*(1 - q_0^N / Q^N) \quad \text{(Nitrogen limitation)} \qquad (6)$$

$$\mu_P = \mu_P^*(1 - q_0^P / Q^P) \quad \text{(Phosphorus limitation)} \qquad (7)$$

where μ_N = specific growth rate under nitrogen limitation;
μ_P = specific growth rate under phosphorus limitation;
q_0^N= minimum nitrogen cell quota;
q_0^P= minimum phosphorus cell quota;
μ_N^*= maximum growth rate obtained by making cell quota of nitrogen (Q^N) infinite; and
μ_P^*= maximum growth rate obtained by making cell quota of phosphorus (Q^P)infinite.

(Multiple nutrient limitation (14))

When limiting factor switches, we have to consider the limiting effect of both nitrogen and phosphorus. Rhee (14) proposed Eq. 8 to take such situations into account. Since it is shown that the Droop type equation is not applicable to non-limiting factors (5), we adopted Eq. 8 to deal with such situations.

$$f_3 = \min[\mu_N, \mu_P] \qquad (8)$$

(Uptake rate for phosphorus (11), (10), (12))

$$V_P = V_{PO_4} = V_{max}^{PO_4} \frac{S_{PO_4}}{K_S^{PO_4} + S_{PO_4}} \qquad (9)$$

where $V_{max}^{PO_4}$ = maximum phosphate uptake rate;
$K_S^{PO_4}$ = half saturation concentration for phosphate uptake; and
S_{PO_4} = ambient phosphate concentration.

(Uptake rate for nitrogen (10), (12), (13))

$$V_N = V_{NH_4} + V_{NO_3}$$
$$= V_{max}^{NH_4} \frac{S_{NH_4}}{K_S^{NH_4} + S_{NH_4}} + \frac{1}{1 + \frac{S_{NH_4}}{K_I}} V_{max}^{NO_3} \frac{S_{NO_3}}{K_S^{NO_3} + S_{NO_3}} \qquad (10)$$

where $V_{max}^{NH_4}$, $V_{max}^{NO_3}$ = maximum uptake rates of NH_4^+ and NO_3^-, respectively;
$K_S^{NH_4}$, $K_S^{NO_3}$ = half saturation concentrations for $NH_4^+$and NO_3^-,respectively;
K_I = inhibition constant; and
S_{NH_4}, S_{NO_3} = ambient concentrations of NH_4^+ and NO_3^-, respectively.

Growth model of *S. costatum*

The growth of *S. costatum* is also represented by a quota type formulation (Eqs. 6 and 7). Nutrient uptake kinetics are described by a Michaelis-Menten-type formula (Eqs. 9 and 10). However, the nutrient uptake formula for *S. costatum* does not consider how ammonium interferes with the uptake of nitrate as the formula for *C. antiqua* does. *S. costatum* has a higher specific growth rate than *C. antiqua* but it is not capable of DVM. All other functions representing the growth and nutrient uptake are the same for *S. costatum* and *C. antiqua* except for irradiation. Eq. 11 describes the irradiation function for S. costatum.

$$f_2(I) = 1 - \exp(-I / I_k) \qquad (11)$$

By combining two ecologically different phytoplankton models, we can assess the competition and succession under the influence of changing environmental conditions. Parameter values are summarized in Table 1.

Table 1 Summary of the parameter values

	P				N				
	q_0 (pmol/cell)	K_s (μM)	V_{max} (pmol/cell·h)	μ_{max} (1/d)	q_0 (pmol/cell)	K_s (μM)	V_{max} (pmol/cell·h)	μ_{max} (1/d)	
S. costatum	0.002	0.1	0.003	1.752	0.04	1.5	0.02	1.752	
C. antiqua	0.62	1.76	0.14	0.93	7.8	2.81	0.91	0.78	(NO_3)
						2.19	2.02		(NH_4)

From Nakamura (10), (12), (13) and Lehman et al. (8)

Eq. 12 calculates the irradiation in a water column. Since only *C. antiqua* accumulates at the surface, we are only concerned with the cell concentration of *C. antiqua* when calculating the attenuation parameter.

$$I(z) = I_0 \cdot \exp(-kz) \qquad (12)$$

where

I_0 = Irradiance at the surface;

$k = k_0 + \alpha \times 4.7 \times 10^{-7} \times N(z)$;

$\alpha = 5.0$;

$N(z)$= *C. antiqua* cell concentration;

k_0 = attenuation constant of sea water; and

z = depth (m).

Calibration Results

We have applied our model to *C. antiqua* red tide-forming experiments (3 cases) carried out using a large axenic culture tank at the National Institute for Environmental Studies (NIES). Experiments were done following a procedure in which the medium was well mixed by bubbling air for the first several days

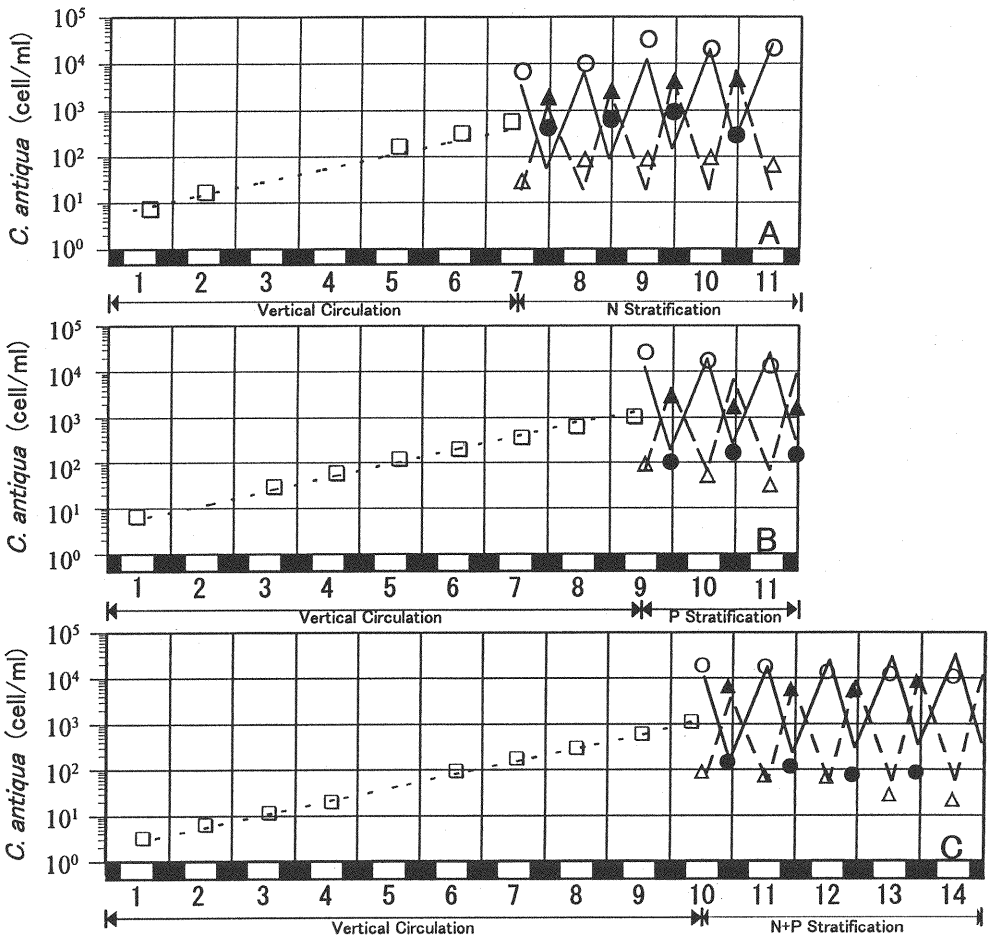

Fig. 2. *C. antiqua* cell concentration under nutrient stratification in the axenic tank.
Observed values are from the surface/daytime(○), surface/night(●), bottom/daytime(△), bottom/night(▲), and the middle(□). Calculated values are for the surface(—), bottom(- -), and middle(···). A. *C. antiqua* cell concentration under N stratification. B. Same for under P stratification. C. Same for under N+P stratification. (Light and dark periods are indicated above day number.)

to allow *C. antiqua* to multiply, and then stopping the mixing. After the bubbling had been shut down, 100 liters of water were withdrawn from the bottom of the column and replaced with nutrient-rich water. Newly replaced water also has higher salinity and cooler temperature (ΔS=2.8‰, ΔT=2℃) (16). Thus, a nutricline was formed on the day of the experiment. During

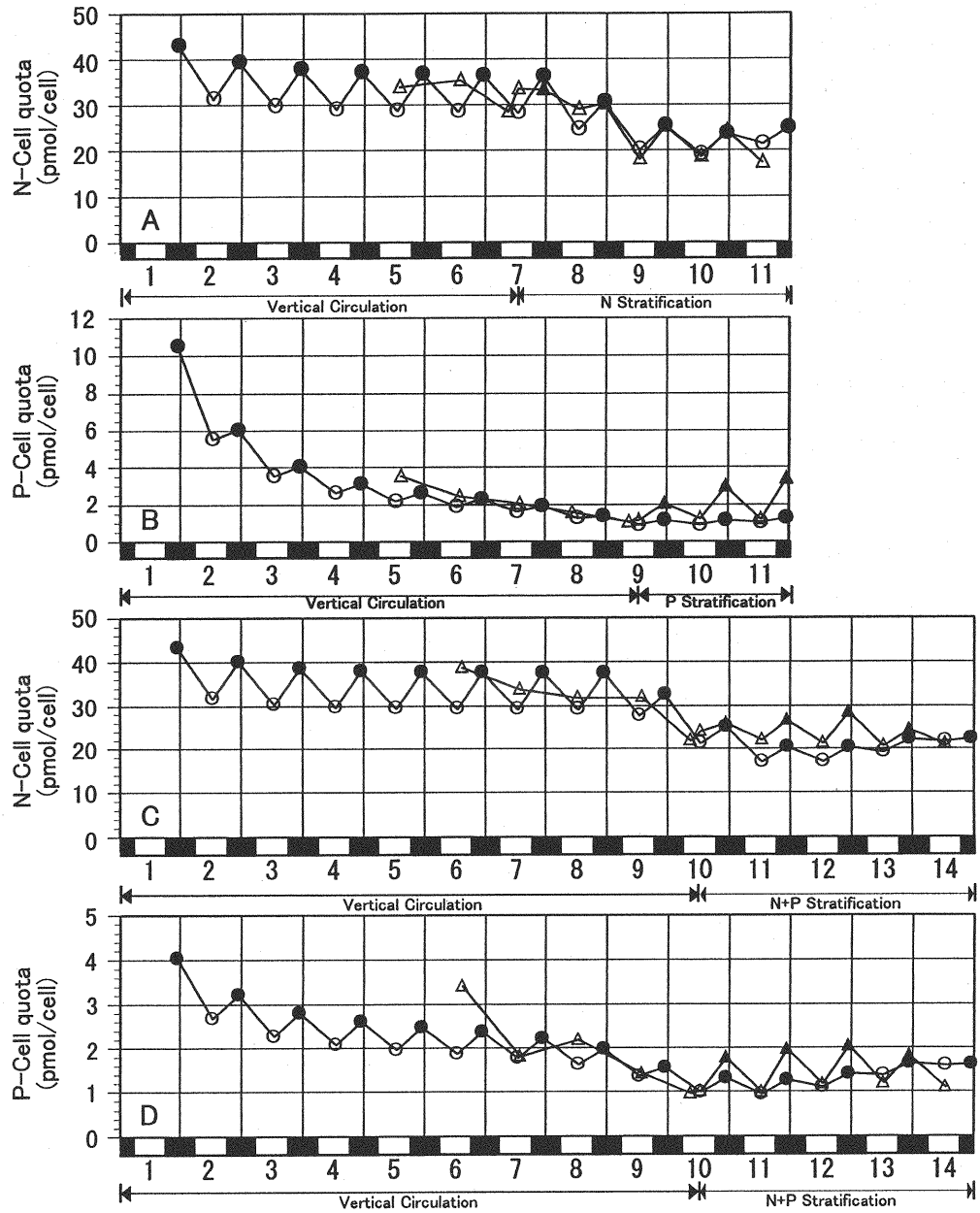

Fig. 3. Nutrient concentration change at the surface and the bottom in the axenic tank. Observed values are from the surface(●) and bottom(▲). Calculated values are for the surface(—) and bottom(- -). A. NO_3^- concentration under N stratification. B. PO_4^{3-} concentration under P stratification. C. NO_3^- concentration under N+P stratification. D. PO_4^{3-} concentration under N+P stratification. (Light and dark periods are indicated above day number.)

experiments, vertical profiles of *C. antiqua* cell concentration, nitrate, phosphate, particulate nitrogen and particulate phosphorus were measured to observe possible changes from *C. antiqua* activity. A detailed description of these experiments is given in Watanabe et al. (16). Model calculations have been done according to the conditions of the experiments.

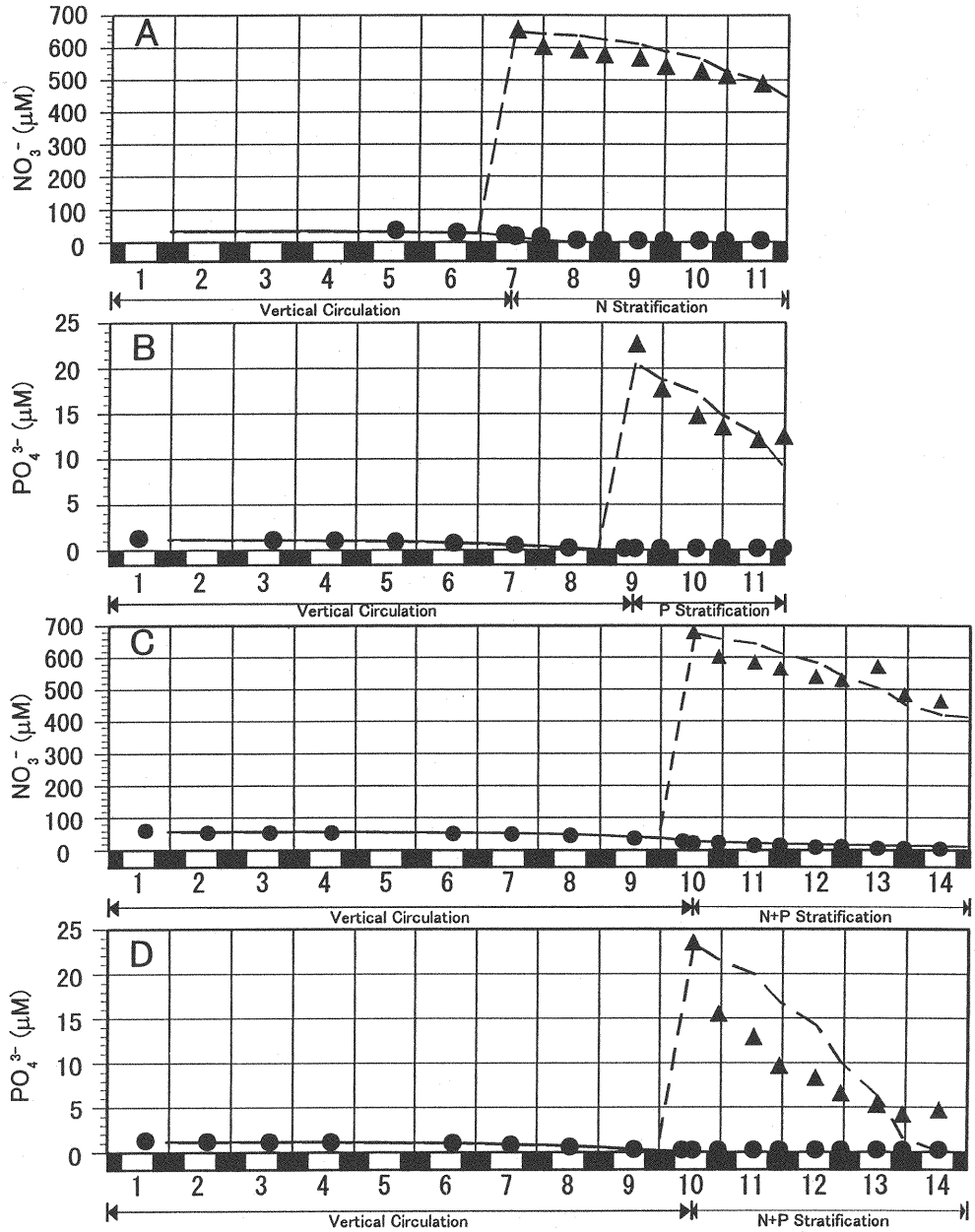

Fig. 4. Intracellular nutrient concentration change in the axenic tank experiments. Observed values are from the surface/daytime(△) and bottom/night(▲). Calculated values are for the surface/daytime (○) and bottom/night(●). A. N cell quota under N stratification. B. P cell quota under P stratification. C. N cell quota under N+P stratification. D. P cell quota under N+P stratification. (Light and dark periods are indicated above day number.)

The calculated *C. antiqua* concentration change is compared with the one measured in Fig. 2. We assumed that cell division occurs once a day based on the experiment, and this assumption seems reasonable from the comparison. Since the column was well mixed due to bubbling for the first several days of the experiment, we compared the values measured at the middle depth with the calculated values. The mixing effect was represented by averaging the calculated results vertically throughout the column at each time step of the calculation (Δ t=0.02h). During the mixing period the calculated results agreed well with the measured ones. After the bubbling had been terminated, *C. antiqua* cells began DVM. Because of this, the vertical profile of *C. antiqua* cells varied depending on the DVM phase. Therefore, we compared the observed and calculated results for 1300 and 2300 h at the surface and at the bottom (Fig. 2). *C. antiqua* cells began to migrate upwards a few hours ahead of the light period and formed a bloom at the surface (1300 h)(16). They began to migrate downwards one to two hours before the light was turned off, and reached the bottom since the column was only 1.5 m high (2300 h)(16). The calculated results agreed well with the observed diel pattern.

Experimental and simulated values of nitrogen cell quota at 1300 h at the surface and at 2300 h at the bottom are compared in Figs. 3(A) and 3(C). The cell quota was obtained by dividing particulate nutrient concentrations by the cell concentration. The nitrogen cell quota decreased to almost half due to cell division and increased thereafter by nutrient uptake. Simulated results reflected this pattern quite well. Although nitrate was depleted at the surface after it was no longer being mixed (Figs. 4(A) and 4(C)), the nitrogen cell quota level continued to increase after cell division because of the nocturnal nutrient uptake at the bottom. Simulated results showed this feature even after nitrogen depleted at the surface, indicating that the model of nitrogen uptake was appropriate after cells began DVM. The measured and simulated results for phosphorus cell quota variation also agreed well (Figs. 3(B), 3(D)). Thus, the nutrient uptake kinetics for both nitrogen and phosphorus were shown to be reasonable in comparison with the experiment results.

The calculated bottom nitrate concentration of the medium was lower than the one measured after day 13 of N+P stratification case; however, the pattern of variation agreed well (Fig. 4(C)). Calculated and measured phosphorus concentration profiles of the medium also agreed well (Figs. 4(B), 4(D)).

These results prove that the *C. antiqua* ecological model is capable of representing unique ecological features. The DVM model was proved to be reasonable by comparison with the experiment results obtained by Watanabe et al (17)(1).

Simulation results and discussion

The simulation was conducted to analyze the effects of surface mixing and nutricline depth on the growth of *Chattonella antiqua*, taking into account its competition with *Skeletonema costatum*. In a 20 m deep bay, initial conditions provided *C. antiqua* concentration of 5 cells/ml for the bottom 1-m layer and 5 cells/ml of *S. costatum* throughout the water column. We conducted 4 simulations varying the nutricline depth and the surface mixing intensity. Nutricline was set at depths of 10 m and 6 m. We conducted two simulations for each nutricline depth. The intensity of the surface mixing varied: thoroughly mixed within the 5-m surface layer, no additional mixing to the diffusive effect by dispersion coefficient. Initial nutrient concentrations were set as follows:

Surface PO_4^{3-} = 0.04 μM, NO_3^- = 0.2 μM, NH_4^+ = 0.4 μM;

Bottom PO_4^{3-} = 0.3 μM, NO_3^- = 4.0 μM, NH_4^+ = 2.0 μM.

Simulation results were compared using the vertical profiles of two plankton species at 1400 h on day 30 from the beginning of the calculation. When the nutricline was formed at a depth of 10 m and no mixing was assumed at the surface, *S. costatum* almost disappeared because the cells sank. The *C. antiqua* concentration was minimal, because the cells were unable to reach the nutrient-rich bottom water. On the other hand, when we completely mixed the 5-

m surface layer, *S. costatum* cells were sustained and able to stay at the surface long enough to compensate for the loss from sinking. Since *S. costatum* was able to take up nutrients at the surface in this case, *C. antiqua* growth was further suppressed (Fig. 5).

When the nutricline was formed at a depth of 6 m and no mixing was assumed at the surface, *C. antiqua* was able to migrate deeper than the nutricline during the night, and nutrients were available for cells by nocturnal nutrient uptake. Thus, *C. antiqua* was able to grow, in spite of the

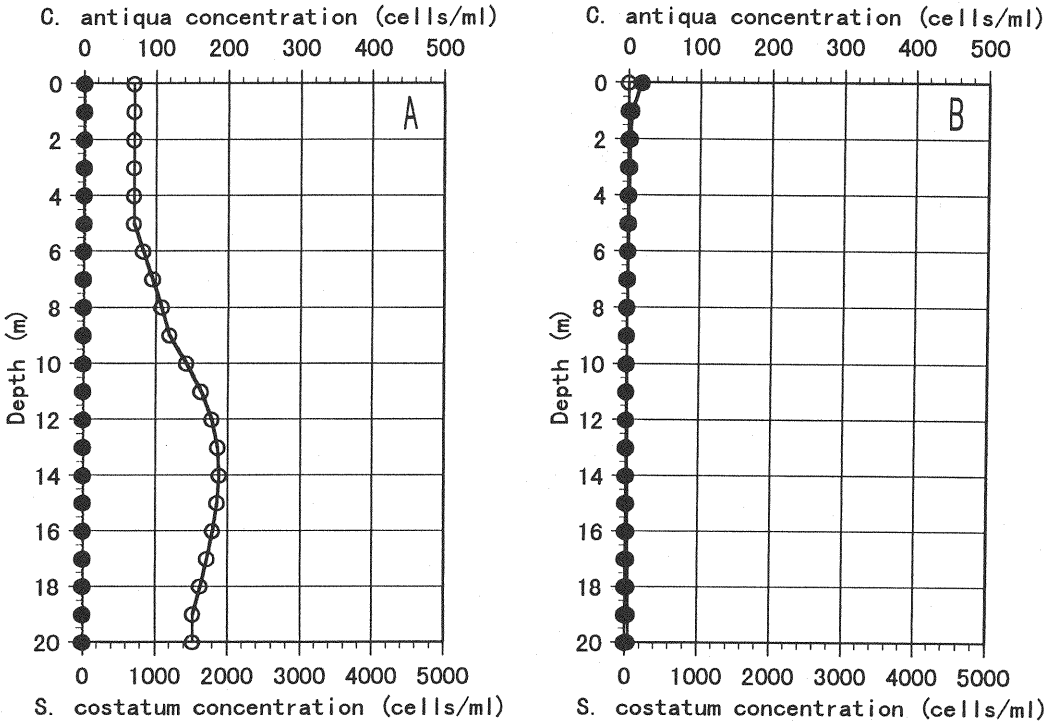

Fig. 5. Vertical profile for *C. antiqua* and *S. costatum* depending on the mixing intensity (Nutricline depth = 10 m)
C. antiqua (●), *S. costatum* (○)
A. 5m surface mixing condition
B. No mixing condition

nutrient depletion at the surface, to the level required to form a red tide. However, mixing suppressed the growth of *C. antiqua* by hindering their migration and increasing the nutrient uptake by *S. costatum* (Fig. 6).

These results seem consistent with field observations, where factors such as surface mixing and nutricline depth determine the dominant phytoplankton species. Diatoms like *S. costatum*, which are not motile, favor mixed conditions and will become dominant because of their fast specific growth rate. On the other hand, *C. antiqua*, which cannot grow as fast as *S. costatum*, is favored when stratification is stable and nutricline is shallow on account of its ability for DVM.

Each phytoplankton species has its own strategy to survive in the face of competition. DVM and nocturnal nutrient uptake, which are unique ecological features of *C. antiqua*, enable the species to become dominant when surface mixing is suppressed and a shallow nutricline is formed. *S. costatum*, which is not motile, has a rapid specific growth rate and has adapted ecologically to counter sinking. The sinking rate of a particle can be represented by Stokes' law as follows,

$$v_a = \frac{2gr^2}{9}\frac{(\rho'-\rho)}{\nu\cdot\phi_r}$$

where ϕ_r is a shape coefficient.

The density of a *S. costatum* cell was determined according to the experiment done by Watanabe (15). Although *S. costatum* cells are denser than ordinary seawater, the species reduces its sinking rate by increasing its shape coefficient by connecting cells like a chain. Since we did not consider this effect in the present study, we may have overestimated the sinking rate of *S. costatum*. Future research aimed at evaluating such an effect and the relationship between surface mixing and sinking rate will refine the model further.

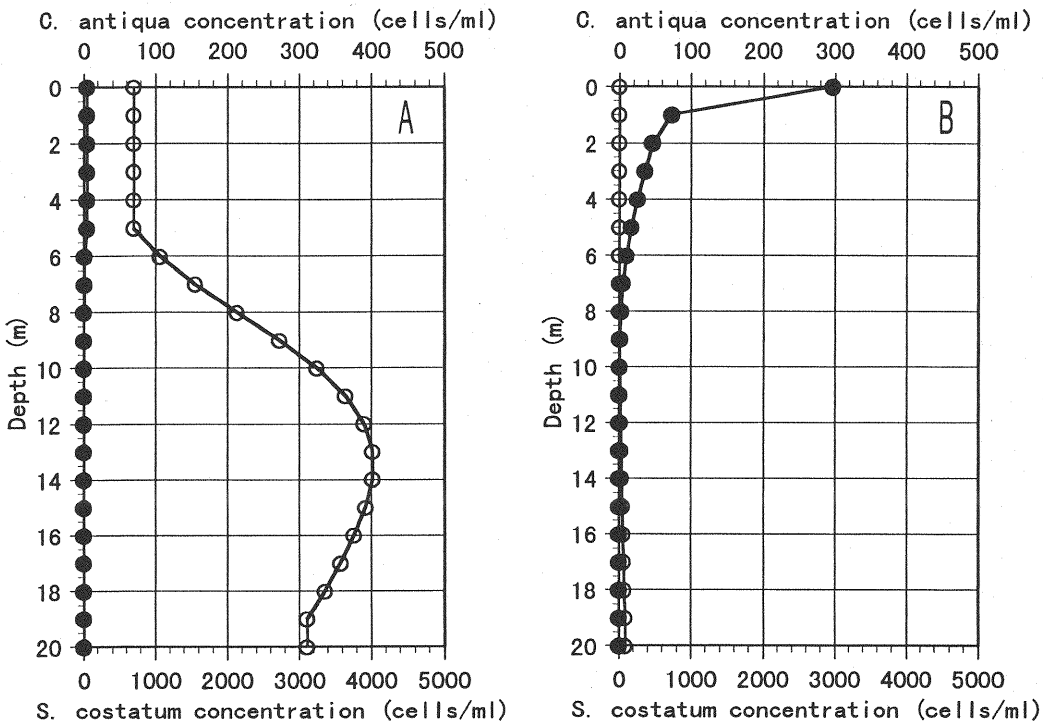

Fig. 6. Vertical profile for *C. antiqua* and *S. costatum* depending on the mixing intensity (Nutricline depth = 6 m)
C. antiqua (●), *S. costatum* (○)
A. 5m surface mixing condition
B. No mixing condition

Conclusion

We have developed an ecological model for two phytoplankton species (*C. antiqua* and *S. costatum*) to assess the effects that physicochemical marine features, such as surface mixing and the nutricline depth, have on the competition and succession of these two species. Simulation results showed that the above factors determine which species will be dominant. Since our model reflects the outcome of the ecologically unique features of these species, it can be used to explain the causes leading to the dominance of one species. Our model shows that the requirements for a *C. antiqua* red tide outbreak are a shallow nutricline and suppressed surface mixing.

REFERENCES

1. Amano, K., M. Watanebe, K. Kohata, and S. Harada : Conditions necessary for *Chattonella antiqua* red tide outbreaks, Limnol. Oceanogr., Vol. 43, pp.117-128, 1998.
2. Bannister, T. T.: Quantitative description of steady state, nutrient-saturated algal growth including adaptation, Limnol. Oceanogr., Vol.24, pp.76-96, 1979.
3. Droop, M. R. : Vitamin B12 and marine ecology: the response of *Monochrysis lutheri*, J. Mar. Biol. Assoc. U. K., Vol.46, pp.659-671, 1966.
4. Droop, M. R. : Some thoughts on nutrient limitation in algae, J. Phycol., Vol.9, pp.264-272, 1973.
5. Elrifi, I. R. and D. H. Turpin: Steady-state luxury consumption and the concept of optimum nutrient ratios: A study with phosphate and nitrate limited *Selenastrum minutum* (Chlorophyta). J. Phycol. Vol.21, pp. 592-602, 1985.
6. Kishi M., S. Ikeda, T. Hirano and A. Nishimura : Numerical simulation model of the ecology of red tide forming phytoplankton, Engan-kaiyo-kenkyu Note, Vol.22, pp.109-118, 1985, (In Japanese with English abstract).
7. Lamanna, C. and M. F. Mallette : Basic Bacteriology, The Williams and Wilkins Co., Baltimore, MD, 1965.
8. Lehman, J. T., D. B. Botkin and G. E. Likens: The assumptions and rationales of a computer model of phytoplankton population dynamics, Limnol. Oceanogr., Vol.20, pp.343-364, 1975.
9. Mickelson, M. J., H. Maske and R. C. Dugdale : Nutrient-determined dominance in multispecies chemostat cultures of diatoms, Limnol. Oceanogr., Vol.24, pp.298-315, 1979.
10. Nakamura, Y. and M. M. Watanabe : Nitrate and phosphate uptake kinetics of *Chattonella antiqua* grown in light/dark cycles, J. Oceanogr. Soc. Japan, Vol. 39, pp.167-170, 1983.
11. Nakamura Y. : Alkaline phosphatase activity of *Chattonella antiqua* and *Heterosigma akashiwo*, Res. Rep. Natl. Inst. Environ. Stud., Jpn., No.80, pp.67-72, 1985 (In Japanese with English abstract).
12. Nakamura, Y. : Kinetics of nitrogen- or phosphorus- limited growth and effects of growth conditions on nutrient uptake in *Chattonella antiqua*, J. Oceanogr. Soc. Japan, Vol.41, pp.381-387, 1985a.
13. Nakamura, Y. : Ammonium uptake kinetics and interactions between nitrate and ammonium uptake in *Chattonella antiqua*, J. Oceanogr. Soc. Japan, Vol.41, pp.33-38, 1985b.
14. Rhee, G. Y. : Effects of N:P atomic ratios and nitrate limitation on algal growth, cell composition and nitrate uptake, Limnol. Oceanogr., Vol.23, pp.10-25, 1978.
15. Watanabe, M: The diurnal variations in the cell densities of *Olisthodiscus luteus* and *Skeletonema costatum*, Res. Rep. Natl. Inst. Environ. Stud., N.30, pp.143-154, 1982.
16. Watanabe, M., K. Kohata and T. Kimura : Diel vertical migration and nocturnal uptake of nutrients by *Chattonella antiqua* under stable stratification, Limnol. Oceanogr., Vol.36, pp.593-602, 1991.
17. Watanabe, M., K. Kohata, T. Kimura, T. Takamatsu, S. Yamaguchi and T. Ioriya : Generation of a *Chattonella antiqua* bloom by imposing a shallow nutricline in a mesocosm, Limnol. Oceanogr., Vol.40, pp.1447-1460, 1995.
18. Yamazaki, H and D. Kamykowski : The vertical trajectories of motile phytoplankton in a wind-mixed water column, Deep-Sea Research, Vol.38, pp.219-241, 1991.

APPENDIX - NOTATION

The following symbols are used in this paper:

A_j = horizontal cross-sectional area of control volume;

C_i = concentration of component i;

C_i^0 = concentration of component i (inflow);

E = vertical dispersion coefficient;

g = gravitational acceleration;

I = irradiance;

I_0 = irradiance at the surface;

I_k = irradiance at which growth rate reaches a maximum;

I^* = threshold irradiation for growth;

k_0 = attenuation constant of sea water;

K_I = inhibition constant;

$K_S^{NH_4}$ = half saturation concentration for ammonia uptake;

$K_S^{NO_3}$ = half saturation concentration for nitrate uptake;

$K_S^{PO_4}$ = half saturation concentration for phosphate uptake;

m_1 = dimensionless parameter characteristic for algal species;

m_2 = dimensionless parameter characteristic for algal species;

n = dimensionless parameter characteristic for algal species;

N_0 = cell concentration before division;

N_1 = cell concentration after division;

q_0^N = minimum nitrogen cell quota;

q_0^P = minimum phosphorus cell quota;

Q^N = cell quota of nitrogen;

Q^P = cell quota of phosphorus;

Q_V = vertical flowrate;

r = radius of a particle;

S_{NH_4} = ambient ammonia concentration;

S_{NO_3} = ambient nitrate concentration;

S_{PO_4} = ambient phosphate concentration;

T_{max} = maximum temperature for growth;

T_{opt} = optimum temperature for growth;

T^* = threshold temperature for growth;

U_i = horizontal inflow velocity;

U_o = horizontal outflow velocity;

V_a = sinking rate of a particle;

V_M = DVM velocity;

$V_{max}^{NH_4}$ = maximum ammonia uptake rate;

$V_{max}^{NO_3}$ = maximum nitrate uptake rate;

$V_{max}^{PO_4}$ = maximum phosphate uptake rate;

V_N = nitrogen uptake rate;

V_{NO_3} = nitrate uptake rate;

V_{NH_4} = ammonia uptake rate;

V_P = phosphorus uptake rate;

V_{PO_4} = phosphate uptake rate;

W_S = settling velocity;

z = depth;

μ = specific growth rate;

μ_N = specific growth rate under nitrogen limitation;

μ_P = specific growth rate under phosphorus limitation;

μ_N^* = maximum growth rate obtained by making cell quota of nitrogen (Q^N) infinite;

μ_P^* = maximum growth rate obtained by making cell quota of phosphorus (Q^P)infinite;

ν = kinematic viscosity;

ρ = density of ambient water;

ρ' = density of a particle; and

ϕr = shape coefficient.

(Received February 27, 1998; revised May 6, 1998)